Journal of Environmental Management 268 (2020) 110340

Contents lists available at ScienceDirect

Journal of Environmental Management

journal homepage: http://www.elsevier.com/locate/jenvman

Research article

Designing silica xerogels containing RTIL for CO_2 capture and CO_2/CH_4 separation: Influence of ILs anion, cation and cation side alkyl chain length and ramification

Leonardo M. dos Santos [a], Franciele L. Bernard [a], Bárbara B. Polesso [b], Ingrid S. Pinto [a], Claudio C. Frankenberg [a], Marta C. Corvo [c], Pedro L. Almeida [c,d], Eurico Cabrita [e], Sandra Einloft [a,b,*]

[a] School of Technology, Pontifical Catholic University of Rio Grande do Sul, PUCRS, Brazil
[b] Post-Graduation Program in Materials Engineering and Technology, Pontifical Catholic University of Rio Grande do Sul, PUCRS, Brazil
[c] CENIMAT|i3N, Dep. Ciência dos Materiais, Faculdade de Ciências e Tecnologia, Universidade NOVA de Lisboa, Caparica, Portugal
[d] ISEL, ADF, Rua Conselheiro Emídio Navarro 1, Lisboa, Portugal
[e] UCIBIO, Dep.Química, Faculdade de Ciências e Tecnologia, Universidade NOVA de Lisboa, Caparica, Portugal

ARTICLE INFO

Keywords:
CO_2 separation
Silica xerogels
Ionic liquids
Natural gas

ABSTRACT

CO_2 separation from natural gas is considered to be a crucial strategy to mitigate global warming problems, meet product specification, pipeline specs and other application specific requirements. Silica xerogels (SX) are considered to be potential materials for CO_2 capture due to their high specific surface area. Thus, a series of silica xerogels functionalized with imidazolium, phosphonium, ammonium and pyridinium-based room-temperature ionic liquids (RTILs) were synthesized. The synthesized silica xerogels were characterized by NMR, helium pycnometry, DTA-TG, BET, SEM and TEM. CO_2 sorption, reusability and CO_2/CH_4 selectivity were assessed by the pressure-decay technique. Silica xerogels containing IL demonstrated advantages compared to RTILs used as separation solvents in CO_2 capture processes including higher CO_2 sorption capacity and faster sorption/desorption. Using fluorinated anion for functionalization of silica xerogels leads to a higher affinity for CO_2 over CH_4. The best performance was obtained by SX- [bmim] [TF_2N] (223.4 mg CO_2/g mg/g at 298.15 K and 20 bar). Moreover, SX- [bmim] [TF_2N] showed higher CO_2 sorption capacity as compared to other reported sorbents. CO_2 sorption and CO_2/CH_4 selectivity results were submitted to an analysis of variance and the means compared using Tukey's test (5%).

1. Introduction

Natural gas contains high levels of impurities such as carbon dioxide (CO_2) which must be removed to meet product specification, pipeline specifications and diminish global warming. Chemical absorption processes with aqueous alkanolamines solutions have been used commercially for removal of CO_2 from natural gas (Kazemi et al., 2016; Washim Uddin and Hägg, 2012).

The common alkanolamines used for chemical absorption processes are monoethanolamine (MEA), diethanolamine (DEA), triethanolamine (TEA) and methyl diethanolamine (MDEA) (McGurk et al., 2017; Yu, 2012). The use of these compounds in CO_2 capture has demonstrated some drawbacks, including high equipment corrosion rate, large energy penalty for solvent regeneration and amines degradation/evaporation (McGurk et al., 2017; Yu, 2012).

Recent works using adsorbents or mixing them in matrix membranes for CO_2/CH_4 separation were reported (Hasegawa and Matsumoto, 2017; Shafie et al., 2017; Yuan et al., 2016). However, the industrial application of these materials have some drawbacks such as low selectivity (activated carbon) (Huang et al., 2003), thermal instability (zeolites) (Yuan et al., 2016), brittleness and dependence of chemical and thermal stability with the polymeric matrix (Vinoba et al., 2017).

Room-temperature ionic liquids (RTILs), a special class of green solvents, have been proposed as a promising alternative to overcome some problems associated with the use of alkanolamines. It is due to their potential as environmentally friendly solvents, high thermal

* Corresponding author. School of Technology, Pontifical Catholic University of Rio Grande do Sul, PUCRS, Brazil.
E-mail address: einloft@pucrs.br (S. Einloft).

https://doi.org/10.1016/j.jenvman.2020.110340
Received 2 September 2019; Received in revised form 24 January 2020; Accepted 24 February 2020
Available online 14 May 2020

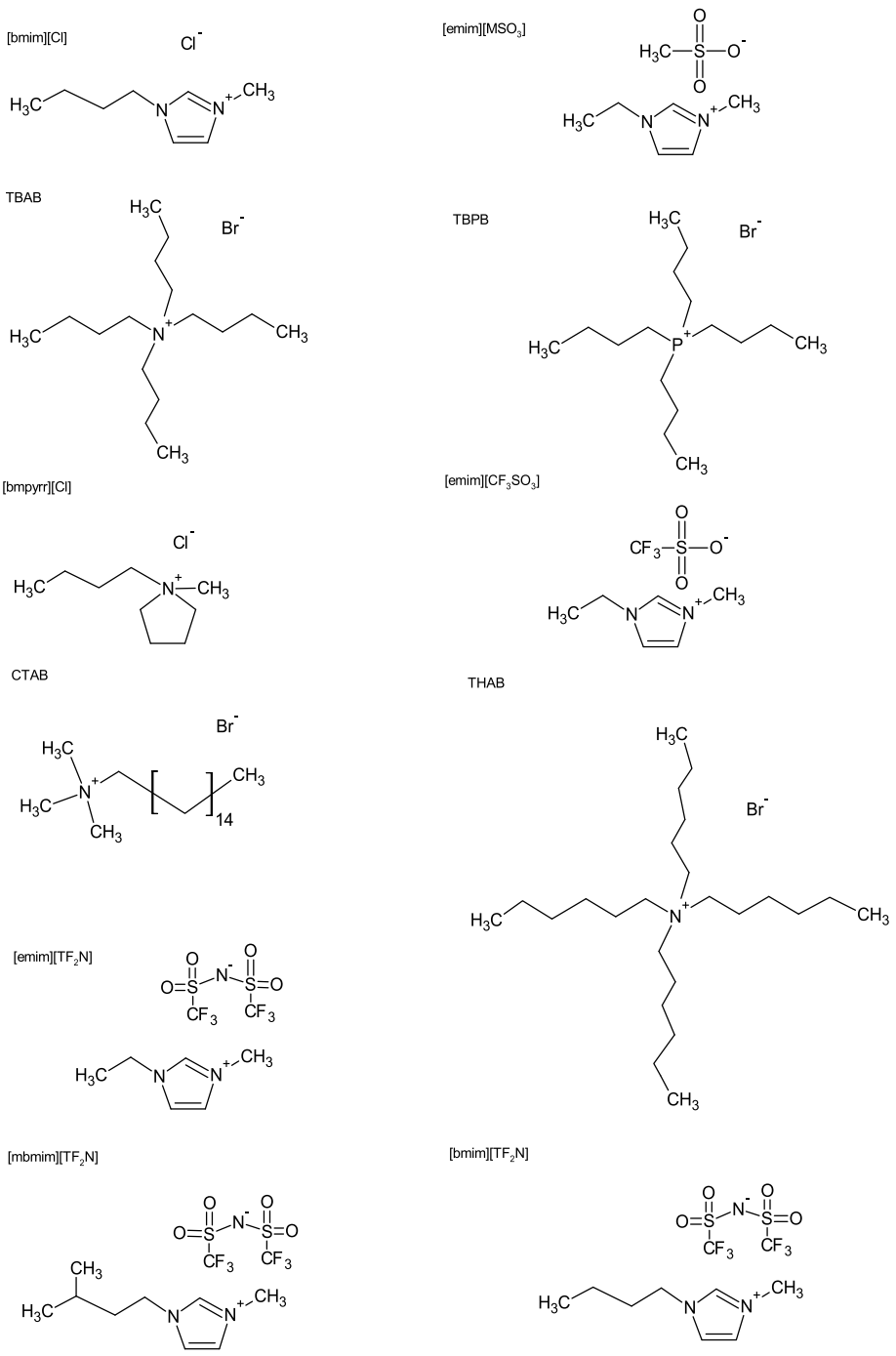

Fig. 1. ILs structures used for silica xerogels synthesis.

stability, non-flammability, negligible vapor pressure, large versatility, recyclability and selective CO_2 absorption in gas mixtures (Hasib-ur-Rahman et al., 2010; Seo et al., 2014). However, the RTILs high viscosity can represent a barrier to implementation in CO_2 capture plants (Hasib-ur-Rahman et al., 2010). One solution for overcoming this disadvantage is the use of RTILs in silica by sol gel method.

Silica xerogels and aerogels containing ionic liquids have been reported in literature for different applications in material science such as catalyst, encapsulation, optical and electronic materials, and nanostructure formation templates.

The sol–gel process synthesized silica containing ILs presents large surface area, high porosity and narrow pore size distribution (Donato et al., 2009).

We report here the synthesis and characterization of several functional silica xerogels using ionic liquids (ILs). ILs cation and anion structure influence on the CO_2 sorption capacity and CO_2/CH_4 separation was investigated. The cations evaluated include imidazolium, phosphonium, ammonium and pyridinium - based ILs. The anions methanesulfonate ([CH3SO3−]), trifluoromethyl sulphonate ([CF3SO3−]),bis(trifluoromethane)sulfonamide([TF2N−]) chloride ([Cl-]) and bromide ([Br-]) were used in this work.

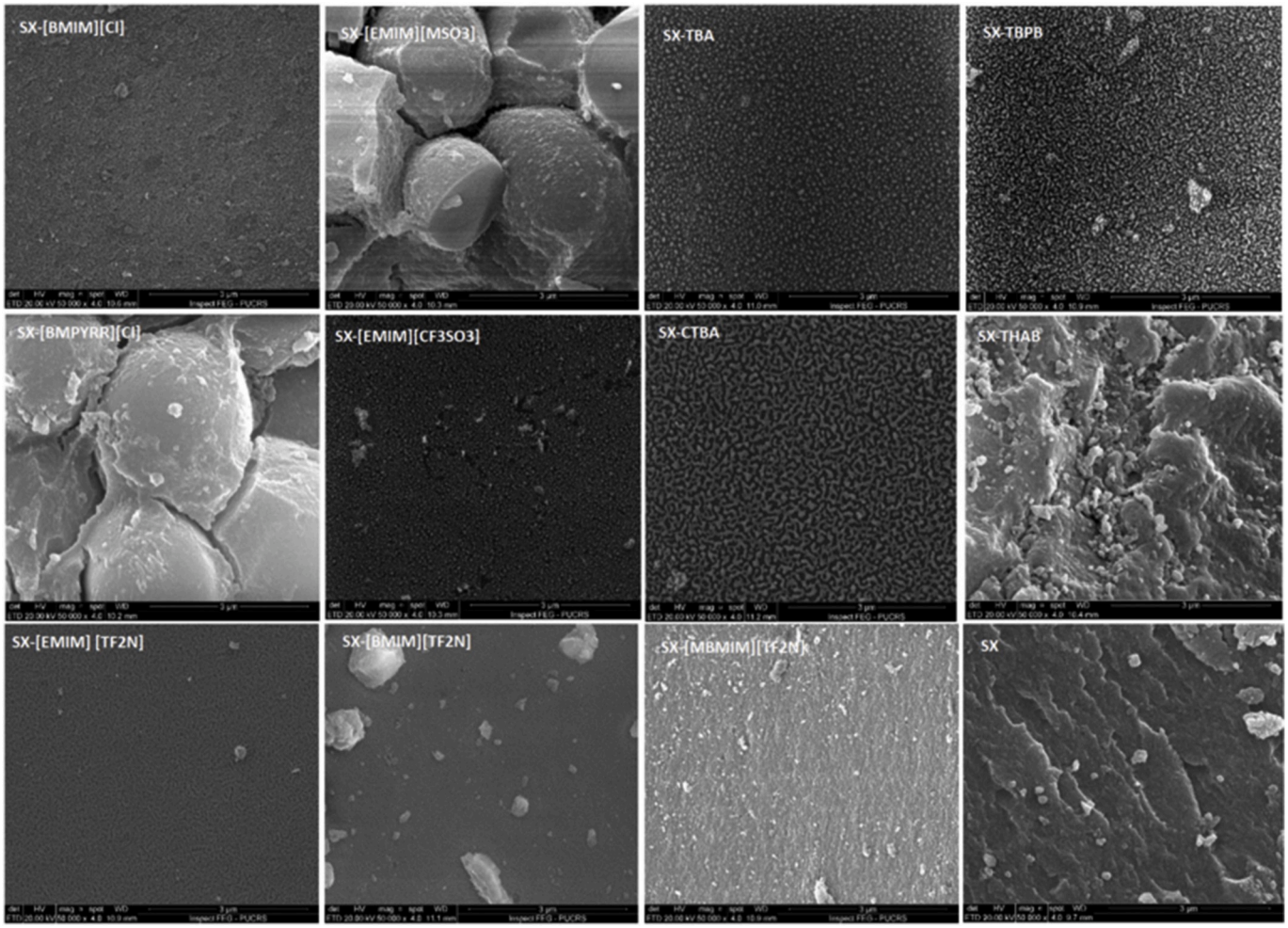

Fig. 2. Micrographs obtained for silica xerogel and silica xerogels functionalized with IL (magnification 20.000×).

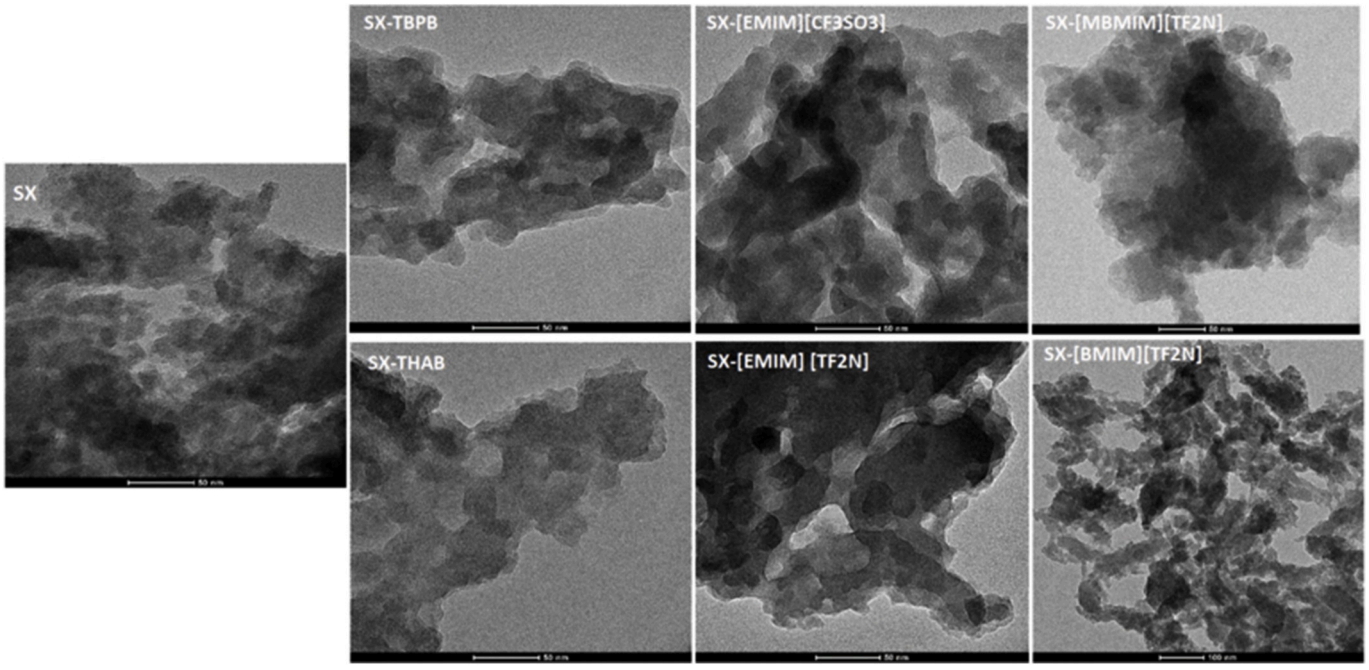

Fig. 3. TEM images of silica xerogel and silica xerogels functionalized with IL.

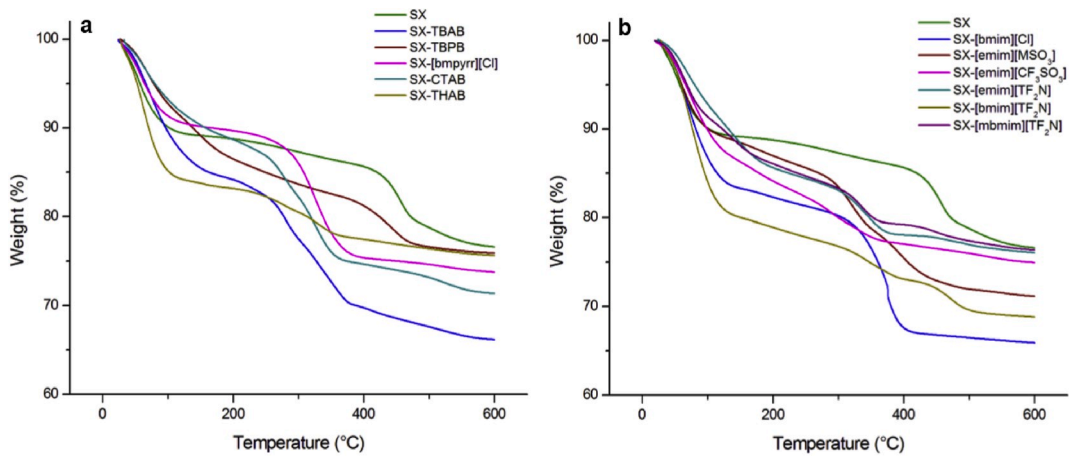

Fig. 4. TGA of silica xerogel and silica xerogels functionalized with IL.

Table 1
Structural properties of silica xerogels.

	Densities (g/cm3)		Porosity (%)	Pore volume (cm^3/g)	Pore radius (nm)	BET (m^2/g)
	Bulk density	Skeleton density				
SX	0.7686	2.37	67.57	0.24	1.18	595
SX – [bmim][Cl]	0.8196	2.67	69.30	0.10	1.63	116
SX – [emim][MSO3]	0.7477	2.69	72.20	0.16	1.83	180
SX – TBAB	0.8025	3.16	74.60	0.13	1.24	223
SX – TBPB	0.7791	2.67	70.82	0.25	1.27	388
SX – [bmpyrr][Cl]	0.8461	2.15	60.65	0.07	1.33	100
SX – [emim][CF3SO3]	0.6985	2.69	74.03	0.19	1.32	282
SX – CTAB	0.7617	2.30	66.88	0.11	1.50	141
SX – THAB	0.8946	2.23	59.88	0.22	1.58	278
SX –[emim][TF2N]	0.7434	1.85	59.82	0.33	1.20	546
SX –[bmim][TF2N]	0.8236	1.86	55.72	0.24	1.41	343
SX –[mbmim][TF2N]	0.5120	1.82	71.87	0.26	1.35	378

2. Experimental

2.1. Materials

Tetraethyl orthosilicate (TEOS, Merck, 98%, USA), sodium fluoride (NaF, Synth, 99% Brazil), polyvinylic acid (PVA, Dinâmica, 95%, Brazil), hydrochloric acid (HCl, 37%, Anidrol, Brazil), carbon dioxide 4.0 (CO_2, 99,80%, White Martins, Brazil), standard mixture (CO_2/CH_4 35 mol % of CO_2 and CH4 balance), White Martins, Brazil) were used as received without further purification. Tetrabutylammonium bromide (TBAB, NEON, 99%, Brazil), tetrabutylphosphonium bromide (TBPB, Sigma Aldrich, 98%,USA), 1-butyl-1-methylpyrrolidinium chloride (BMPYRR, Sigma Aldrich, 99%, USA), 1-ethyl-3-methylimidazolium trifluoromethanesulfonate ([EMIM][CF_3SO_3], Merck, 98%, USA), 1-ethyl-3-methylimidazolium methanesulfonate ([EMIM][MSO_3], Merck, 95%, USA), Hexadecyltrimethylammonium bromide (CTAB, Sigma Aldrich, 99%, USA), Tetrahexylammonium bromide (THAB, Sigma Aldrich, 99%, USA) and, 1-butyl-3-methylimidazolium derivatives were prepared according to the literature procedure (Dupont et al., 2002). The synthesized [bmim][Cl], [bmim][TF_2N], [emim][TF_2N], [mbmim][TF_2N] were characterized by Proton Nuclear Magnetic Resonance (^{1}H-NMR), in Varian spectrophotometer, VNMRS 300 MHz, using DMSO-d_6 as solvent and 5 mm glass tubes. ^{1}H-NMR (300 MHz, DMSO-d_6, 25 °C), δ (ppm): 1.01 (m, CH_3), 1.29 (m, CH_2CH_3), 1.83 (m, CH_2), 3.97 (s, CH_3), 4.25 (t, CH_2N), 7.79 (s, H5), 7.91 (s, H(4)), 9.48 (s, H(2)). [bmim][TF_2N] - ^{1}H-NMR (300 MHz, DMSO-d_6) δ (ppm): 9,11 [s, ^{1}H]; 7,78 [d, ^{1}H, J = 1,7 Hz]; 7,86 [d, 1H, J = 1,6 Hz]; 4,22 [t, 2H, J = 7, 2 Hz]; 3,91 [s, 3H]; 1,87–1,68 [m,2H, J = 14,9; 7,4 Hz]; 1,29 [dt, 2H, J = 14,7; 7,3 Hz]; 0,90 [t, 3H, J = 7,3 Hz]. [emim][TF_2N] - ^{1}H-NMR (300 MHz, DMSO-d_6) δ (ppm): 9,15 [s, 1H]; 7,78 [d, 1H, J = 1,8 Hz]; 7,70 [d, 1H, J = 1,6 Hz]; 4,19 [m, 2H, J = 7,3 Hz]; 3,85 [s, 3H]; 1,35 [t, 3H, J = 7,3 Hz]. [mbmim][TF_2N] - ^{1}H-NMR (300 MHz, DMSO-d_6) δ (ppm): 9,13 [s, 1H]; 7,79 [d, 1H, J = 1,7 Hz]; 7,70 [d, ^{1}H,J = 1,8 Hz]; 4,24 [t, 2H]; 3, 85 [s, 3H]; 1,69 [m, 2H, J = 7,2 Hz]; 1,51 [m, 1H, J = 13,4; 6,5 Hz]; 0,92 [d, 6H].

2.2. Silica xerogel synthesis

Silica xerogels containing ILs were synthesized following procedures adapted from literature (Vidinha et al., 2006; VIdinha et al., 2008). A series of samples were prepared by mixing 25 mg IL, 2.28 mmol TEOS, PVA (4.64 g/L), NaF (0.20 g/L) and 6.86 mmol distilled water. The reaction mixture was stirred and placed in ice bath or in the refrigerator until gelation. The gels obtained were kept at 35 °C for 24 h and washed several times with acetone and n-pentane. Finally, silica xerogels were dried at 35 °C for 24 h. The ILs structures used are shown in Fig. 1 A silica xerogel sample *(SX) was also prepared without IL*. Silica xerogels containing IL*s were labeled as SX-IL. For example, SX-[bmim][Cl] means s*ilica xerogel containing 1-Bu*tyl-3-methylimidazolium chlori*de IL.

2.3. Characterization of silica xerogels

Structural elucidation of neat samples was carried out by solid state NMR (SS NMR) techniques. 13C MAS and 29Si MAS NMR spectra were acquired with a 7 T (300 MHz) AVANCE III Bruker spectrometer operating respectively at 75 MHz (13C) and 60 MHz (29Si), equipped with a BBO probe head. The samples were spun at the magic angle at a frequency of 5 kHz in 4 mm-diameter rotors at room temperature. The 13C MAS NMR experiments were acquired with proton cross polarization (CPMAS) with a contact time of 1.2 ms, and the recycle delay was 2.0 s. The single pulse 29Si MAS NMR experiments were acquired with a recycle delay of 10.0 s.

The samples morphology was determined with a field emission scanning electron microscope (FESEM) using Inspect F50 equipment (FEI Instruments) in secondary electrons mode and transmission electron microscopy (TEM) using a Tecnai G2 T20 FEI operating at 200 kV. Surface area, pore radius and pore volume were determined by Brunauer-Emmett-Teller (BET) and Barrett-Joyner-Halenda (BJH)

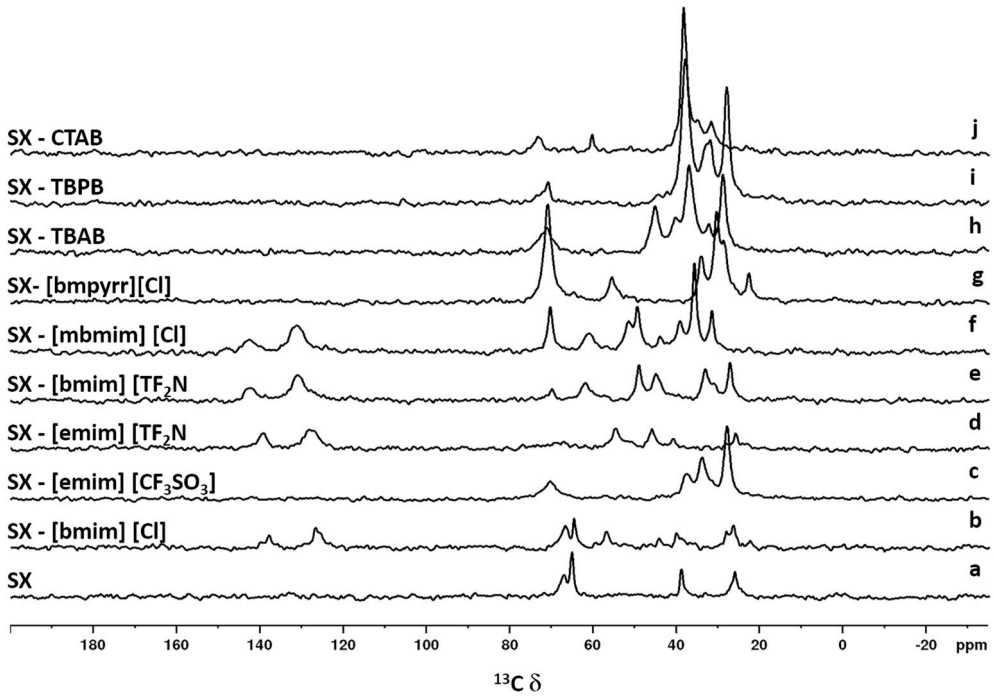

Fig. 5. 13C CPMAS NMR spectra of silica xerogel (a) and silica xerogels functionalized with ILs: (b) SX – [bmim] [Cl]; (c) [emim] [CF_3SO_3]; (d) SX –[emim] [TF_2N]; (e) SX –[bmim] [TF_2N]; (f) SX –[mbmim] [TF_2N]; (g) SX- [bmpyrr][Cl]; (h) SX – TBAB; (i) SX – TBPB; (j) SX-CTAB.

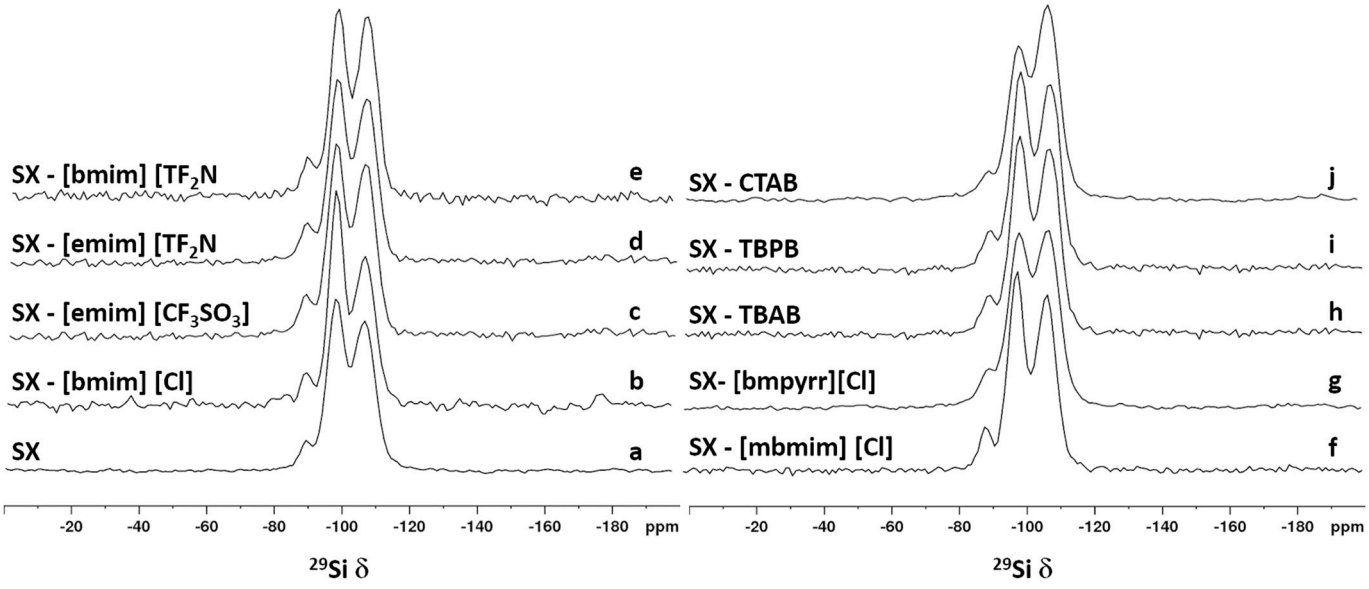

Fig. 6. 29Si MAS NMR spectra of silica xerogel (a) and silica xerogels functionalized with ILs: (b) SX – [bmim] [Cl]; (c) [emim] [CF_3SO_3]; (d) SX –[emim] [TF_2N]; (e) SX –[bmim] [TF_2N]; (f) SX –[mbmim] [TF2N]; (g) SX- [bmpyrr][Cl]; (h) SX – TBAB; (i) SX – TBPB; (j) SX-CTAB.

methods, respectively using NOVA 4200e. The bulk density was determined by measuring the volume and weight of dispersed powder in a container under the influence of gravity. The skeletal density (true density) was obtained by helium pycnometry (Ultrafoam™1200e, Quantachrome Instruments). Porosity (%) was calculated theoretically using the values of bulk density and skeletal density following procedure from literature(Tokudome et al., 2009). Thermogravimetric analysis (TGA) curves were obtained using a TA Instrument SDT-Q600, the temperature range was set at 25 °C–600 °C with a heating rate of 20 °C/min and under a nitrogen atmosphere.

2.4. CO_2 uptake measurement

CO_2 sorption capacity was determined using a dual-chamber gas sorption cell by pressure-decay technique (Koros and Paul, 1976). A detailed description of experimental equipment and procedure is available in our previous publications (Bernard et al., 2018, 2017; Fernández Rojas et al., 2017). The experiments were carried out in triplicate. Samples (1.0–1.2 g) were loaded in the sorption chamber and degassed under vacuum (10^{-3} mbar) at 298.15 K during 30 min. CO_2 sorption tests were carried out at 298.15 K with pressure ranging from 1

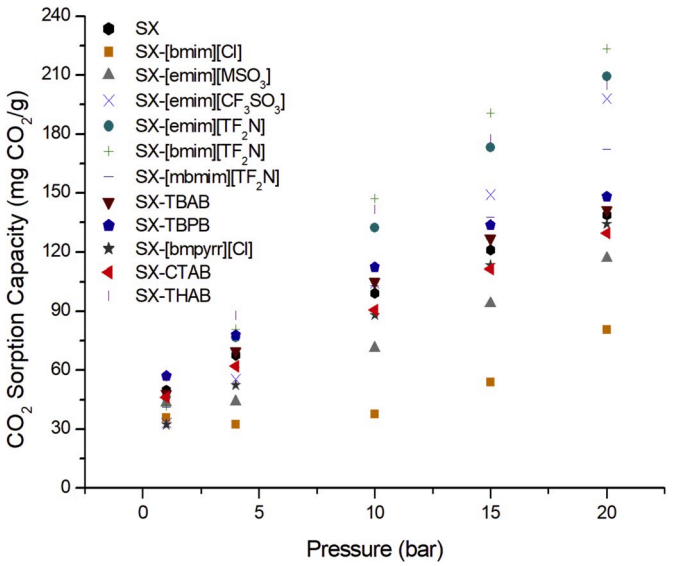

Fig. 7. Silica xerogel and silica xerogels functionalized with IL CO_2 sorption values at 298.15 K.

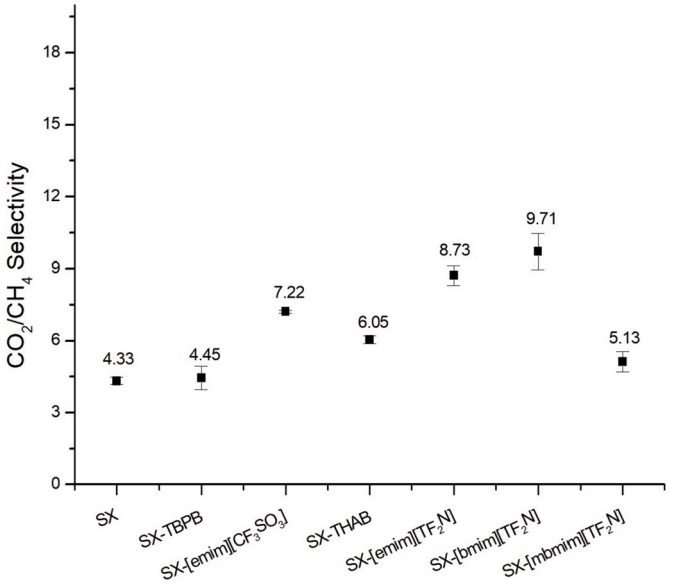

Fig. 8. CO_2/CH_4 selectivity of silica xerogel and silica xerogels functionalized with IL at 20 bar and 298.15 K.

to 30 bar.

2.4.1. Sorption/desorption tests

Sorption/desorption tests were performed by using CO_2. Then CO_2 sorption/desorption cycles were performed in the silica xerogel containing IL. CO_2 sorption was evaluated at 298.15 K and 20 bar and desorption under vacuum (10-3 mbar) at 298.15 K during 30 min. CO_2 sorption was also probed in NMR using a similar procedure as previously described (Corvo et al., 2013). Briefly, using a high pressure (HP) NMR cell from DAEDALUS INNOVATIONS, LLC, 150 mg of xerogel were equilibrated at 298.15 K and 20 bar CO_2. The system was considered to have reached equilibrium when the pressure was unchanged with time for 12 h. The HP NMR cell was then transferred to the NMR spectrometer using a protective polycarbonate structure. 13C NMR was performed in a Bruker Avance III 400 operating at 400.15 MHz for hydrogen and 100.61 MHz for carbon, using an inverse gated 1H decoupled pulse

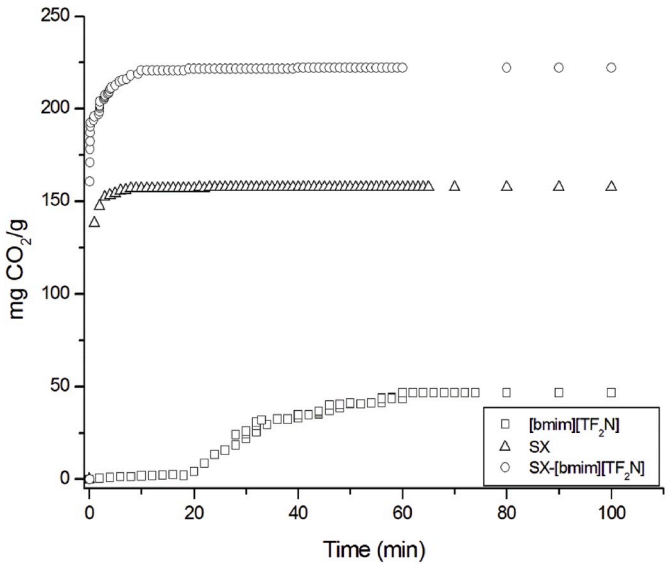

Fig. 9. CO_2 sorption kinetics (□) [bmim][TF_2N] IL (Δ) SX (○) SX-[bmim][TF_2N]. CO_2 sorption values at 20 bar and 298.15 K.

sequence with a relaxation delay of 25 s, collecting 128 transients and 64 K data points.

2.5. CO_2/CH_4 separation selectivity

The separation of CO_2 from CO_2/CH_4 gas mixture (35 mol % of CO_2 and CH_4 balance) was also assessed in a dual-chamber gas sorption cell similar to Koros et al. (Koros and Paul, 1976). The samples (1.0–1.2 g) were also previously degassed under vacuum (10 -3 mbar) at 298.15 K during 30 min. The CO_2/CH_4 selectivity tests were performed at 298.15 K and 20 bar. The apparatus and full experimental procedure were described elsewhere (Azimi and Mirzaei, 2016; Duczinski et al., 2018; Fernández Rojas et al., 2017).

2.6. Statistical analysis

Data were analyzed with one–way analysis of variance (ANOVA) and with Tukey-Kramer multiple comparison test, using SPSS (version 18.0). The significance level of all statistical tests was fixed at 0.05.

3. Results and discussion

3.1. Silica xerogel characterization

Silica xerogel and silica xerogels functionalized with IL morphologies can be seen in Fig. 2. Micrographs showed a change in silica xerogel morphology after the addition of IL. Formation of larger spherical particles than SX were observed for SX-[bmim][Cl], SX-TBAB, SX-TBPB, SX-[emim][CF_3SO_3], SX-CTBA, SX-[emim][TF_2N], SX-[bmim][TF_2N] and SX-[mbmim][TF_2N]. Silica xerogels functionalized with [bmpyrr][Cl] and [emim][MSO_3] showed formation of much larger spherical particles than all other samples. Silica xerogel functionalized with THAB promoted the formation of highly aggregated particles.

Fig. 3 shows TEM images of silica xerogel and silica xerogels functionalized with IL that presented a greater CO_2 sorption capacity than SX (see Fig. 7). The particle size of silica xerogel tend to increase after functionalization with IL. Functionalized silica xerogels particles showed larger particles than SX.

3.2. silica xerogel thermal analysis

TGA analysis (Fig. 4) was used to evaluate thermal stability of silica

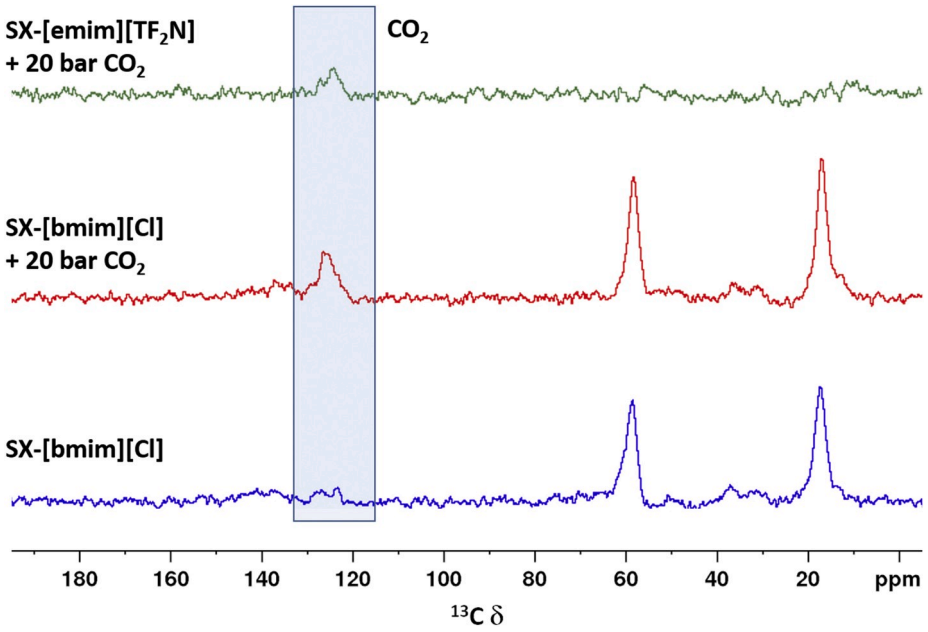

Fig. 10. HP-NMR of xerogels −13C NMR inverse gated spectra of silica xerogels functionalized with IL, without and with 20 bar CO_2.

xerogels. All samples presented three main degradation stages (Fig. 4a and b). The first weight loss between 35 °C and 170 °C is attributed to water and solvent evaporation (Sun et al., 2017). The second weight between 210 °C and 370 °C is associated to the dissociation of IL and/or PVA (Bryaskova et al., 2013; Patil and Murthy, 2017) and the third thermal event between 380 °C and 585 °C is probably due to silane groups degradation (Si-OC2H5) (Duczinski et al., 2018; Sun et al., 2017).

3.3. Silica xerogel structural properties

Table 1 summarizes the structural properties of synthesized xerogels. Calculated porosity from bulk density and skeleton density for SX was 67.57% while the porosity values of silica xerogel containing IL varied in the range from 55.72% to 74.60% indicating that the presence of IL produce small changes in silica xerogel porosity. This behavior may result from low IL concentration (5%wt in TEOS) used in silica xerogel synthesis. On the other hand, the addition of IL in silica xerogel promotes a reduction in surface area and pore volume as seen in Table 1. The pore radius changes from 1.18 nm to 1.83 nm depending on the starting IL.

3.4. ^{13}C CPMAS and ^{29}Si NMR of silica xerogel

The functionalized xerogel samples were further analyzed using NMR spectroscopy to study the outcome of each polymerization and provide an evidence of the incorporation of the ionic liquid moiety in the xerogel. In the 13C CPMAS NMR spectra of silica xerogel it's possible to observe chemical shifts from CH3, CH2 and OCH2 groups at 15; 29 and 57–59 ppm, respectively (Fig. 5 a). In the IL functionalized xerogels additional chemical shifts reveal the presence of the IL moieties (Fig. 5-b-i), more specifically, in the imidazolium ILs the aromatic ring carbons at 120–130 ppm and the aliphatic chain chemical shifts between 20 and 40 ppm. In the ammonium ILs the presence of the aliphatic chain is also observable at 20–30 ppm.

In the ^{29}Si NMR spectra (Fig. 6), three distinct resonances for siloxane are observable [Q^n = $Si(OSi)_n(OH)_{4-n}$, n = 2–4], with Q^2 appearing at −95; Q^3 at −104 and Q^4 at −113 ppm.

In Table S1 the relative areas of the Q^n bands are presented in Table S1, and it's possible to observe that in IL functionalized xerogels Q^2 is decreased while Q^3 and Q^4 tend to increase. The Q^4/Q^3 ratio is a consequence of the degree of condensation of TEOS in the xerogel. From Table S1 analysis, some samples show a higher Q^4/Q^3 ratio when compared to SX, which means that in these cases TEOS must be more reticulated, namely in SX – TBAB and SX – CTAB. All the imidazolium TF_2N derivatives exhibit an intermediate degree of reticulation, similar among each other. SX – [bmim] [Cl], SX -[bmpyrr][Cl] and SX – [emim] [CF_3SO_3] have an opposite effect showing a slight decrease in reticulation. Comparing the Q^4/Q^3 ratios with the pore volume and radius (Table 1), it is interesting to notice that only with the more hydrophobic ILs such as imidazolium TF_2N derivatives, the observed reticulation is very similar or slightly higher than SX, a trend that is followed by the respective pore volume and radius.

3.5. CO_2 uptake for silica xerogel samples-influence of cation, anion and side alkyl chain

CO_2 sorption capacity results are shown in Fig. 7. Statistical analysis (see Table S2) showed that the experimental results were reproducible within an average experimental error < 0.05. Gas sorption capacity increases significantly as CO_2 partial pressure increases. SX presented a CO_2 sorption value of 49.9 mgCO_2/g (1 bar) and 138 mgCO_2/g (20 bar). The SX sorption capacity is attributed to silanol groups distributed on the silica xerogel surface along with the largest specific surface area (595 m2 g−1) (Witoon et al., 2011) when compared to silica xerogels containing IL (e.g. SX-[bmim][TF2N] = 343 m2 g−1). At lower pressures, CO_2 sorption values obtained for silica xerogels functionalized with IL and SX sample varied from 32.4 to 57.2 mgCO_2/g (see Fig. 7). At higher pressures SX-[bmim][TF_2N], SX-[emim][TF_2N], SX-[mbmim][TF_2N], SX-[emim][CF_3SO_3], SX-[THAB] and SX-[TBPB] samples presented high CO_2 sorption capacity (e.g. SX-[bmim][TF_2N] = 223.4 mg CO_2/g at 20 Bar) compared to SX sample. RTILs have a strong affinity to CO_2 (Hasib-ur-Rahman et al., 2010; Seo et al., 2014) and the lower CO_2 sorption capacity from SX-[bmim][Cl], SX-[emim][MSO_3], SX-[bmpyrr][Cl], SX-[TBAB] and SX-[CTBA] is probably associated with the reduction of specific surface area and pore volume for lower values than 278 m2 g−1 and 0.19 cm3 g−1 (see Table 1). Xerogels textural properties are a consequence of the reticulation, which depends on the IL nature. IL

functionalized SX exhibiting pore volumes lower than 0.19 cm^3 g^{-1} and a high degree of reticulation perform generally worse than SX, towards CO_2 sorption. This is the case for SX-[bmim][Cl], SX-[emim][MSO_3], SX-[bmpyrr][Cl] and SX-[CTBA]. However, samples that maintain the pore volume equal to, or larger than 0.19 cm^3 g^{-1} and a similar degree of reticulation as SX have a high CO_2 sorption capacity. This is the case of SX-[bmim][TF_2N], SX-[emim][TF_2N], SX-[mbmim][TF_2N], SX-[TBPB] and SX-[TBAB]. Our results show that CO_2 sorption capacity is possibly influenced by IL type and textural properties (specific surface area and pore volume), resulting from a compromise between pore volume, reticulation and the IL nature.

Experimental and simulation studies have shown that the nature of anion has stronger effect on CO_2 solubility than cation. Thus, by varying the substituents of cation and anion, one should be able to design ionic liquids to achieve the desired characteristics needed for high CO_2 solubility (Blanchard et al., 2001; Hasib-ur-Rahman et al., 2010; Sarmad et al., 2017; Zeng et al., 2017). There are numerous publications on CO_2 capture based in ILs (Hasib-ur-Rahman et al., 2010; Sarmad et al., 2017; Zeng et al., 2017). RTILs based on alkyl-imidazolium cations are the most investigated for CO_2 capture application (Anthony et al., 2005, 2002; Blanchard et al., 2001; Brennecke and Gurkan, 2010; Cadena et al., 2004; Privalova et al., 2012). However, different cations including pyrrolidinium, pyridinium, and phosphonium have also been explored in an effort to enhance CO_2 solubility (Mahurin et al., 2012; Sarmad et al., 2017). The functionalization of silica xerogels with RTILs based on phosphonium cation improves CO_2 sorption capacity when compared to other cation. CO_2 sorption capacity of SX-[TBPB] was superior than SX-[TBAB], SX-[bmpyrr][Cl] and SX-[bmim][Cl] as seen in Fig. 7.

ILs anion have a larger influence on CO_2 solubility than cation(Sarmad et al., 2017). It has been also reported that CO_2 solubility is greatest for fluorinated anions ILs (Blanchard et al., 2001). This tendency was also observed in this study for SX-ILs samples. The affinity to CO_2 of functionalized silica xerogel increases with fluorinated anion, i.e. CO_2 sorption followed the general trend of SX-[emim][TF_2N]> SX-[emim][CF_3SO_3]> SX-[emim][MSO_3] (see Fig. 7).

The increase in IL cation alkyl-side chain may result in increased CO_2 solubility because it increases free volume available for CO_2 with a corresponding decrease in cation–anion interactions(Corvo et al., 2015; Hou and Baltus, 2007; Shannon et al., 2012; Shiflett and Yokozeki, 2005). This tendency was observed for silica xerogels functionalized with imidazolium cation, where the increase of the alkyl chain length of the IL cation from ethyl (C2) (SX-[emim][TF_2N] = 209.3 mg CO_2/g at 20 Bar) to butyl (C_4) (SX-[bmim][TF_2N] = 223.4 mg CO_2/g at 20 Bar) improved CO_2 sorption. Silica xerogels functionalized with ammonium cation also showed an increase in CO_2 sorption capacity when increasing the alkyl side chain from C_4 to C_6. When CTBA was used as anion a decrease in CO_2 sorption capacity was observed. This behavior must be related to the alkyl side chain folding, decreasing the free volume available for CO_2 molecule. CO2 sorption followed the general trend of SX-[THAB]> SX-[TBA]> SX-[CTBA] as seen in Fig. 7.

The introduction of branches in IL cation can promote an increase in CO_2 solubility because it results in sponge-like ILs (Corvo et al., 2015). Note that in our case, the insertion of branches in IL cation affected negatively the CO_2 sorption capacity of silica xerogel with investigated IL ([mbmim][TF_2N]). CO_2 uptake of SX-[bmim][TF_2N] (223.4 mg CO_2/g at 20 Bar) was superior than SX-[mbmim][TF_2N] (172.2.4 mg CO_2/g at 20 Bar). Branching of IL cation results in the reduction of silica xerogel specific surface area and pore volume (see Table 1). Results obtained in this work for SX-[bmim][TF_2N] at 20 bar (223.4 mg CO_2/g) were higher than those reported in literature under the same pressure and temperature conditions for materials such as SiO_2 (~62.5 mg CO_2/g) (Safiah et al., 2014), Zeolite 5 A (~160.7 mg CO_2/g) (Singh and Kumar, 2016) and SiO_2 supported with 10% of IL [hmim][TF_2N] (10% [hmim][Tf_2N]-Si) (~117.5 mg CO_2/g) (Safiah et al., 2014).

3.6. CO_2/CH_4 selectivity for silica xerogel samples-influence of cation, anion and side alkyl chain

Seven SX-ILs sorbents were selected for comparative study of CO_2/CH_4 selectivity (Fig. 8 and statistical analysis presented at Table S3). The choice of these sorbents was based on CO_2 sorption capacity (see Fig. 7). It has been reported in literature (Anthony et al., 2002) that Carbon dioxide has the highest solubility and strongest interactions with RTILs compared to the solubility of other gases. This behavior was verified in our experiments where CO_2/CH_4 selectivity tended to increase with insertion of IL into the silica xerogel structure as seen in Fig. 8.

Silica xerogels containing RTILs based on alkyl-imidazolium cations tends to increase the CO_2 selectivity (Fig. 8). Anion fluorination led to a higher affinity for CO_2 over CH_4. Therefore, the selective capacity of silica xerogels for CO_2 over CH_4 can be improved by IL cation alkyl-side chain (SX-([bmim][TF_2N]> [emim][TF_2N]) or increased anion fluorination (SX-([emim][TF_2N]> [emim][CF_3SO_3]). Results obtained for [bmim][TF_2N] and [mbmim][TF_2N] suggest that there are no gains in selectivity with the introduction of branching in the alkyl side chain of the IL cations. The best performance was obtained for SX-[bmim][TF_2N]. Selective capacity of 9.71 for SX-[bmim][TF_2N] is higher compared to composite polyurethane foam/ionic liquids (PUF BF4 40: CO_2/CH_4 selectivity of 1.42 at 30 Bar and 298.15 K) (Fernández Rojas et al., 2017), ILs immobilized on mesoporous silica (MCMRH-IL-B10: CO_2/CH_4 selectivity of 5.56 at 40 Bar and 298.15 K) (Duczinski et al., 2018) and commercial MCM-41-silica (CO_2/CH_4 selectivity of 4.91 at 40 Bar and 298.15 K) (Duczinski et al., 2018).

3.7. Sorption kinetic study and recyclability for sample SX-[bmim][TF_2N]

SX-[bmim][TF_2N] was selected to perform a CO_2 sorption kinetic study and recyclability behavior. SX-[bmim][TF_2N] was submitted to five sorption/desorption cycles (Fig. S1). Silica xerogel functionalized with IL presented reversible CO_2 sorption/desorption performance indicating that CO_2 desorption can be carried out under vacuum at 298.15 K. This result is consistent with a typical physical sorbent behavior.

Higher CO_2 sorption capacity and faster sorption rate was obtained for, SX and SX- [bmim] [TF_2N] compared to RTILs as seen in Fig. 9. SX-[bmim] [TF_2N] required only 2 min to reach 90% of their CO_2 sorption capacity, whereas for [bmim] [TF_2N] IL more than 57 min was needed to reach its total sorption capacity (Fig. 9). This behavior can be associated with the high viscosity of [bmim][TF_2N] IL that results in high resistance to mass transfer (Moya et al., 2016). These results showed that silica xerogels containing IL are attractive sorbents for CO_2 capture processes.

3.8. ^{13}C NMR under CO_2 pressure

To obtain further proof of the presence of CO_2 in the xerogel, pressurized samples were analyzed by ^{13}C NMR (Fig. 10). As this experiment was performed in a liquids probe, the IL signals are too broad to be noticed, as such, besides CO_2, only the O–**C**H_2 and –CH_3 from TEOS can be observed.

The broad CO_2 signal in the ^{13}C NMR spectra is indicative of the confinement of this molecule within the matrix of the xerogel, however it is not possible to quantify the total amount of CO_2, because the only other signals are from TEOS matrix.

4. Conclusion

We presented the synthesis and evaluated CO_2 sorption capacity and CO_2/CH_4 separation performance of several functionalized silica xerogels with different ILs. All xerogels exhibited high thermal stability. The results suggest that silica xerogels containing IL are potential sorbents

for CO_2 removal from natural gas due to their competitive surface areas enriched with ionic functional groups. The anion and cation nature affects the extent of the xerogel reticulation, and consequently the intrinsic properties of the resulting materials. The success in CO_2 uptake relies on a compromise between specific surface area, pore volume and IL type. The increase in IL cation alkyl-side chain or the use of fluorinated anions in the functionalization of silica xerogels may promote increased CO_2 sorption, as well as CO_2/CH_4 selectivity. These sorbents preferentially adsorb CO_2 over CH_4 and can be recovered under vacuum and mild temperatures. Yet, CO_2 sorption kinetic of SX- [bmim] [TF_2N] was superior when compared to [bmim] [TF_2N] IL.

Declaration of competing interest

The authors declare that they have no known competing financial interests or personal relationships that could have appeared to influence the work reported in this paper.

CRediT authorship contribution statement

Leonardo M. dos Santos: Conceptualization, Methodology, Investigation, Writing - original draft. **Franciele L. Bernard:** Conceptualization, Investigation, Methodology. **Bárbara B. Polesso:** Methodology, Investigation. **Ingrid S. Pinto:** Investigation, Validation. **Claudio C. Frankenberg:** Formal analysis. **Marta C. Corvo:** Conceptualization, Methodology, Investigation, Writing - original draft. **Pedro L. Almeida:** Conceptualization, Methodology, Investigation, Writing - original draft. **Eurico Cabrita:** Conceptualization, Methodology, Investigation, Writing - original draft. **Sandra Einloft:** Conceptualization, Methodology, Project administration, Funding acquisition.

Acknowledgments

Sandra Einloft thanks CNPq for research scholarship. This work was partially supported by Portuguese funding through FCT- Fundação para a Ciência e a Tecnologia, Portugal (PTDC/QUI-QFI/31508/2017, RNRMN, PINFRA/22161/2016, co-financed by FEDER through COMPETE 2020, POCI, and PORL and FCT through PIDDAC).

Appendix A. Supplementary data

Supplementary data to this article can be found online at https://doi.org/10.1016/j.jenvman.2020.110340.

References

Anthony, J.L., Maginn, E.J., Brennecke, J.F., 2002. Solubilities and thermodynamic properties of gases in the ionic liquid 1- n -Butyl-3-methylimidazolium hexafluorophosphate. J. Phys. Chem. B 106, 7315–7320. https://doi.org/10.1021/jp020631a.

Anthony, J.L., Anderson, J.L., Maginn, E.J., Brennecke, J.F., 2005. Anion effects on gas solubility in ionic liquids: the journal of physical chemistry B. J. Phys. Chem. B 109, 6366–6374. https://doi.org/10.1021/jp046404l.

Azimi, A., Mirzaei, M., 2016. Experimental evaluation and thermodynamic modeling of hydrate selectivity in separation of CO2 and CH4. Chem. Eng. Res. Des. 111, 262–268. https://doi.org/10.1016/j.cherd.2016.05.005.

Bernard, F.L., Polesso, B.B., Cobalchini, F.W., Chaban, V.V., Do Nascimento, J.F., Dalla Vecchia, F., Einloft, S., 2017. Hybrid alkoxysilane-functionalized urethane-imide-based poly(ionic liquids) as a New platform for carbon dioxide capture. Energy Fuels 31, 9840–9849. https://doi.org/10.1021/acs.energyfuels.7b02027.

Bernard, F.L., Duczinski, R.B., Rojas, M.F., Fialho, M.C.C., Carreño, L.Á., Chaban, V.V., Vecchia, F.D., Einloft, S., 2018. Cellulose based poly(ionic liquids): tuning cation-anion interaction to improve carbon dioxide sorption. Fuel 211, 76–86. https://doi.org/10.1016/j.fuel.2017.09.057.

Blanchard, L.A., Gu, Z., Brennecke, J.F., 2001. High-pressure phase behavior of ionic liquid/{CO$_2$} systems. J. Phys. Chem. B 105, 2437–2444. https://doi.org/10.1021/jp003309d.

Brennecke, J.F., Gurkan, B.E., 2010. Ionic liquids for CO2 capture and emission reduction. J. Phys. Chem. Lett. 1, 3459–3464. https://doi.org/10.1021/jz1014828.

Bryaskova, R., Georgieva, N., Andreeva, T., Tzoneva, R., 2013. Cell adhesive behavior of PVA-based hybrid materials with silver nanoparticles. Surf. Coating. Technol. 235, 186–191. https://doi.org/10.1016/j.surfcoat.2013.07.032.

Cadena, C., Anthony, J.L., Shah, J.K., Morrow, T.I., Brennecke, J.F., Maginn, E.J., 2004. Why is CO2 so soluble in imidazolium-based ionic liquids? J. Am. Chem. Soc. 126, 5300–5308. https://doi.org/10.1021/ja039615x.

Corvo, M.C., Sardinha, J., Menezes, S.C., Einloft, S., Seferin, M., Dupont, J., Casimiro, T., Cabrita, E.J., 2013. Solvation of carbon dioxide in [C4 mim][BF(4)] and [C(4) mim][PF(6)] ionic liquids revealed by high-pressure NMR spectroscopy. Angew Chem. Int. Ed. Engl. 52, 13024–13027. https://doi.org/10.1002/anie.201305630.

Corvo, M.C., Sardinha, J., Casimiro, T., Marin, G., Seferin, M., Einloft, S., Menezes, S.C., Dupont, J., Cabrita, E.J., 2015. A rational approach to CO2 capture by imidazolium ionic liquids: tuning CO2 solubility by cation alkyl branching. ChemSusChem 8, 1935–1946. https://doi.org/10.1002/cssc.201500104.

Donato, R.K., Migliorini, M.V., Benvegnú, M.A., Stracke, M.P., Gelesky, M.A., Pavan, F. A., Schrekker, C.M.L., Benvenutti, E.V., Dupont, J., Schrekker, H.S., 2009. Synthesis of silica xerogels with highly distinct morphologies in the presence of imidazolium ionic liquids. J. Sol. Gel Sci. Technol. 49, 71–77. https://doi.org/10.1007/s10971-008-1829-6.

Duczinski, R., Bernard, F., Rojas, M., Duarte, E., Chaban, V., Vecchia, F.D., Menezes, S., Einloft, S., 2018. Waste derived MCMRH- supported IL for CO 2/CH 4 separation. J. Nat. Gas Sci. Eng. 54, 54–64. https://doi.org/10.1016/j.jngse.2018.03.028.

Dupont, Jairton, Consorti, Crestina S., Suarez, Paulo A.Z., de, R.F., Souza, 2002. Preparation of 1-butyl-3-methyl imidazolium-based RoomTemperature ionic liquids. Org. Synth. 79, 236. https://doi.org/10.15227/orgsyn.079.0236.

Fernández Rojas, M., Pacheco Miranda, L., Martinez Ramirez, A., Pradilla Quintero, K., Bernard, F., Einloft, S., Carreño Díaz, L.A., 2017. New biocomposites based on castor oil polyurethane foams and ionic liquids for CO2 capture. Fluid Phase Equil. 452, 103–112. https://doi.org/10.1016/j.fluid.2017.08.026.

Hasegawa, K., Matsumoto, A., 2017. Role of cation in target adsorption of carbon dioxide from CO2-CH4 mixture by low silica X zeolites. AIP Conf. Proc. 1865 https://doi.org/10.1063/1.4993321.

Hasib-ur-Rahman, M., Siaj, M., Larachi, F., 2010. Ionic liquids for CO2 capture-Development and progress. Chem. Eng. Process. Process Intensif. 49, 313–322. https://doi.org/10.1016/j.cep.2010.03.008.

Hou, Y., Baltus, R.E., 2007. Experimental measurement of the solubility and diffusivity of CO 2 in room-temperature ionic liquids using a transient thin-liquid-film method. Ind. Eng. Chem. Res. 46, 8166–8175. https://doi.org/10.1021/ie070501u.

Huang, H.Y., Yang, R.T., Chinn, D., Munson, C.L., 2003. Amine-grafted MCM-48 and silica xerogel as superior sorbents for acidic gas removal from natural gas. Ind. Eng. Chem. Res. 42, 2427–2433. https://doi.org/10.1021/ie020440u.

Kazemi, A., Joujili, A.K., Mehrabani-zeinabad, A., Hajian, Z., Salehi, R., 2016. Influence of CO2 residual of regenerated amine on the performance of natural gas sweetening processes using alkanolamine solutions. Energy Fuel. 30, 4263–4273. https://doi.org/10.1021/acs.energyfuels.6b00295.

Koros, W.J., Paul, D.R., 1976. Design considerations for measurement of gas sorption in polymers by pressure decay. J. Polym. Sci. Polym. Phys. Ed 14, 1903–1907. https://doi.org/10.1002/pol.1976.180141014.

Mahurin, S.M., Hillesheim, P.C., Yeary, J.S., Jiang, D., Dai, S., 2012. High CO2 solubility, permeability and selectivity in ionic liquids with the tetracyanoborate anion. RSC Adv. 2, 11813. https://doi.org/10.1039/c2ra22342b.

McGurk, S.J., Martín, C.F., Brandani, S., Sweatman, M.B., Fan, X., 2017. Microwave swing regeneration of aqueous monoethanolamine for post-combustion CO2 capture. Appl. Energy 192, 126–133. https://doi.org/10.1016/j.apenergy.2017.02.012.

Moya, C., Alonso-Morales, N., Gilarranz, M.A., Rodriguez, J.J., Palomar, J., 2016. Encapsulated ionic liquids for CO2 capture: using 1-Butyl-methylimidazolium acetate for quick and reversible CO2 chemical absorption. ChemPhysChem 17, 3891–3899. https://doi.org/10.1002/cphc.201600977.

Patil, H.R., Murthy, Z.V.P., 2017. A sol–gel route to synthesize vanadium doped silica through ionic liquid control and methylene blue degradation. Chem. Eng. Res. Des. 124, 134–144. https://doi.org/10.1016/j.cherd.2017.06.006.

Privalova, E.I., Mäki-Arvela, P., Murzin, D.Y., Mikkhola, J.P., 2012. Capturing CO 2 : conventional versus ionic-liquid based technologies. Russ. Chem. Rev. 81, 435–457. https://doi.org/10.1070/RC2012v081n05ABEH004288.

Safiah, M.N., Azmi, B.M., Normawati, M.Y., 2014. CO2 capture using silica and molecular sieve impregnated with [hmim][Tf2N]. Int. J. Chem. Eng. Appl. 5, 342–346. https://doi.org/10.7763/IJCEA.2014.V5.406.

Sarmad, S., Mikkola, J.-P., Ji, X., 2017. Carbon dioxide capture with ionic liquids and deep eutectic solvents: a New generation of sorbents. ChemSusChem 10, 324–352. https://doi.org/10.1002/cssc.201600987.

Seo, S., Simoni, L.D., Ma, M., DeSilva, M.A., Huang, Y., Stadtherr, M.A., Brennecke, J.F., 2014. Phase-change ionic liquids for postcombustion CO2 capture. Energy Fuel. 28, 5968–5977. https://doi.org/10.1021/ef501374x.

Shafie, S.N.A., Man, Z., Idris, A., 2017. Development of polycarbonate-silica matrix membrane for CO2/CH4separation. AIP Conf. Proc. 1891 https://doi.org/10.1063/1.5005462.

Shannon, M.S., Tedstone, J.M., Danielsen, S.P.O., Hindman, M.S., Irvin, A.C., Bara, J.E., 2012. Free volume as the basis of gas solubility and selectivity in imidazolium-based ionic liquids. Ind. Eng. Chem. Res. 51, 5565–5576. https://doi.org/10.1021/ie202916e.

Shiflett, M.B., Yokozeki, A., 2005. Solubilities and diffusivities of carbon dioxide in ionic liquids: [bmim][PF 6] and [bmim][BF 4]. Ind. Eng. Chem. Res. 44, 4453–4464. https://doi.org/10.1021/ie058003d.

Singh, V.K., Kumar, E.A., 2016. Comparative studies on CO2 adsorption kinetics by solid adsorbents. Energy Procedia 90, 316–325. https://doi.org/10.1016/j.egypro.2016.11.199.

Sun, S.-Y., Ge, Y.-Y., Tian, Z.-B., Zhang, J., Xie, Z., 2017. A simple method to ameliorate hierarchical porous structures of SiO2 xerogels through adjusting water contents. Adv. Powder Technol. 28, 2496–2502. https://doi.org/10.1016/j.apt.2017.06.019.

Tokudome, Y., Nakanishi, K., Kanamori, K., Fujita, K., Akamatsu, H., Hanada, T., 2009. Structural characterization of hierarchically porous alumina aerogel and xerogel monoliths. J. Colloid Interface Sci. 338, 506–513. https://doi.org/10.1016/j.jcis.2009.06.042.

Vidinha, P., Augusto, V., Almeida, M., Fonseca, I., Fidalgo, A., Ilharco, L., Cabral, S., JM, Barreiros, S., 2006. Sol–gel encapsulation: an efficient and versatile immobilization technique for cutinase in non-aqueous media. J. Biotechnol. 121, 23–33. https://doi.org/10.1016/j.jbiotec.2005.06.018.

VIdinha, P., Augusto, V., Nunes, J., Lima, J., Cabral, J., Barreiros, S., 2008. Probing the microenvironment of sol–gel entrapped cutinase: the role of added zeolite NaY. J. Biotechnol. 135, 181–189. https://doi.org/10.1016/j.jbiotec.2008.03.018.

Vinoba, M., Bhagiyalakshmi, M., Alqaheem, Y., Alomair, A.A., Pérez, A., Rana, M.S., 2017. Recent progress of fillers in mixed matrix membranes for CO2 separation: a review. Separ. Purif. Technol. 188, 431–450. https://doi.org/10.1016/j.seppur.2017.07.051.

Washim Uddin, M., Hägg, M.-B., 2012. Natural gas sweetening—the effect on CO2–CH4 separation after exposing a facilitated transport membrane to hydrogen sulfide and higher hydrocarbons. J. Membr. Sci. 143–149. https://doi.org/10.1016/j.memsci.2012.08.010, 423–424.

Witoon, T., Tatan, N., Rattanavichian, P., Chareonpanich, M., 2011. Preparation of silica xerogel with high silanol content from sodium silicate and its application as CO2 adsorbent. Ceram. Int. 37, 2297–2303. https://doi.org/10.1016/j.ceramint.2011.03.020.

Yu, C.-H., 2012. A review of CO2 capture by absorption and adsorption. Aerosol Air Qual. Res. https://doi.org/10.4209/aaqr.2012.05.0132.

Yuan, Z., Eden, M.R., Gani, R., 2016. Toward the development and deployment of large-scale carbon dioxide capture and conversion processes. Ind. Eng. Chem. Res. 55, 3383–3419. https://doi.org/10.1021/acs.iecr.5b03277.

Zeng, S., Zhang, X., Bai, L., Zhang, X., Wang, H., Wang, J., Bao, D., Li, M., Liu, X., Zhang, S., 2017. Ionic-liquid-based CO $_2$ capture systems: structure, interaction and process. Chem. Rev. 117, 9625–9673. https://doi.org/10.1021/acs.chemrev.7b00072.